FERROELECTRICS
2021, VOL. 575, 11–17
https://doi.org/10.1080/00150193.2021.1888219

Taylor & Francis
Taylor & Francis Group

Electronic band structures of $NdFe_3(BO_3)_4$ and $NdGa_3(BO_3)_4$ crystals: ab initio calculations

S. Krylova[a], I. Gudim[a], A. Aleksandrovsky[a], A. Vtyurin[a,b], and A. Krylov[a]

[a]Kirensky Institute of Physics FRC KSC SB RAS, Krasnoyarsk, Russia; [b]Siberian Federal University, Krasnoyarsk, Russia

ABSTRACT

$NdFe_3(BO_3)_4$ and $NdGa_3(BO_3)_4$ crystals are of great interest due to their physical properties. For example, $NdFe_3(BO_3)_4$ crystal demonstrates magnetodielectric and magnetopiezoelectric effects, and $NdGa_3(BO_3)_4$ crystal possesses luminescent and nonlinear optical properties. In this work, the properties of these materials are calculated by the plane-wave pseudo-potential method based on density functional theory. The structures of the crystals are optimized. The electronic structure of $NdFe_3(BO_3)_4$ and $NdGa_3(BO_3)_4$ are calculated.

ARTICLE HISTORY
Received 17 August 2020
Accepted 30 December 2020

KEYWORDS
Borates; ab initio calculation; electronic bands; crystal structure

1. Introduction

The $NdFe_3(BO_3)_4$ and $NdGa_3(BO_3)_4$ crystals belong to the family of rare-earth trigonal borates with the huntite structure. The borate crystals have become the objects of intensive experimental research in connection with the possibilities of practical application as active laser materials, phosphors, and matrices for the introduction of optically active ions [1–3]. As a rule, these materials are multiferroics [4, 5]. They have high chemical and thermal stability and mechanical strength.

Different scientific groups grew crystals of $NdFe_3(BO_3)_4$ and $NdGa_3(BO_3)_4$ for further research [6–8]. Some studies on the magnetic properties of $NdFe_3(BO_3)_4$ crystal were conducted [9–11]. The $NdFe_3(BO_3)_4$ and $NdGa_3(BO_3)_4$ crystal spectral properties were investigated [12, 13]. $NdGa_3(BO_3)_4$ crystal has luminescent properties [12]. Also, the phonon spectra of $NdFe_3(BO_3)_4$ crystal were studied [10, 11, 14, 15].

The experimental study of complex crystal structures requires an interpretation that cannot be carried out without modeling these materials at the microscopic level. First-principle calculations are often used to describe the structural and vibrational properties of the crystals [16, 17]. The best results in describing the band structure and crystal lattice, can be achieved using methods of the density functional theory.

2. Calculation

The theoretical calculations were carried out by the plane-wave pseudo-potential method based on DFT using the Cambridge Serial Total Energy Package code

CONTACT A. Krylov shusy@iph.krasn.ru

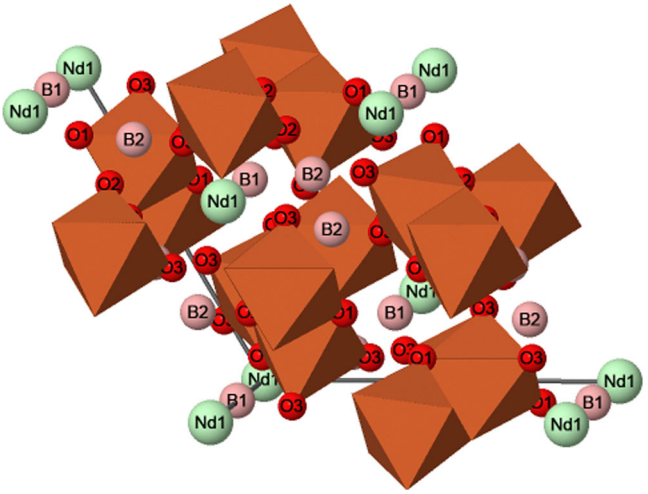

Figure 1. The crystal structure of $NdFe_3(BO_3)_4$: ions of Nd – in light green, ions of B – in pink, ions of O – in red, Fe polyhedra - in orange colors.

(CASTEP) [18]. We used the generalized gradient approximation (GGA) with the Perdew - Burke – Ernzerhof for solids (PBE sol) functional [19]. The calculation was carried out using the algorithm of the minimization method of Bruden, Fletcher, Goldfarb, and Shannon (BFGS) [20]. Lattice constants and atom coordinates have been optimized by minimizing the total energy. Through a series of convergence studies regarding cutoff energies and k-points, cutoff energies were set to $E_{cut} = 880$ eV, and integration in the K-space above the Brillouin zone was performed using a 3k3x3 k-point Monkhorst-Pack mesh [21]. The convergence was within 1.0×10^{-7} eV/atom.

3. Results and discussion

Pseudoatomic calculations were performed for orbitals in $NdFe_3(BO_3)_4$ crystal: B – 2s2, 2p1; O – 2s2, 2p4; Fe – 3s2, 3p6, 3d6, 4s2; Nd – 4f4, 5s2, 5p6, 6s2. The calculation in $NdGa_3(BO_3)_4$ crystal were performed for orbitals: B – 2s2, 2p1; O – 2s2, 2p4; Ga – 3d10, 4s2, 4p1; Nd – 4f4, 5s2, 5p6, 6s2. $NdGa_3(BO_3)_4$ and $NdFe_3(BO_3)_4$ crystals belong to the class of trigonal symmetry (symmetry group *R32* (No. 155)). The Wyckoff positions for Nd, B, Ga (Fe), and O are 3a, 3 b, 9d, 18f, and 9e, respectively. The main structural elements are GaO_6 or FeO_6 octahedra, BO_3 triangles, and NdO_6 triangular prisms.

BO_3 groups are in the layers, and Ga (Fe) atoms are in helicoidal chains. The structures of $NdFe_3(BO_3)_4$ and $NdGa_3(BO_3)_4$ crystals are presented in Figures 1 and 2, respectively. Geometry optimization allows us to refine the geometry of a three-dimensional periodic system to obtain a stable structure. This is done by performing an iterative process, in which the coordinates of the atoms and the cell parameters are adjusted so that the total energy of the structure is minimized. Geometry optimization is based on reducing the calculated forces and stresses until they become less than certain convergence tolerances. The geometry optimization process usually results in a model structure being very similar to the actual structure. To obtain a stable geometric structure,

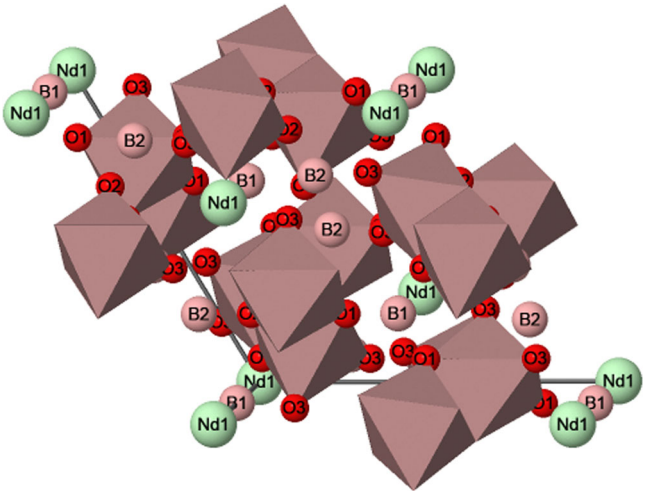

Figure 2. The crystal structure of $NdGa_3(BO_3)_4$: ions of Nd – in light green, ions of B – in pink, ions of O – in red, Ga polyhedra - in brown colors.

we performed structural optimization with gradient approximation (GGA: PBE sol) for determining the internal atomic coordinates and structure parameters. The functional PBEsol (GGA) has been developed specifically to improve the description of exchange in solids, resulting in better structures and energetics for densely packed solids and their surfaces.

The obtained lattice parameters are in good agreement with the experimental data and other calculations for $NdGa_3(BO_3)_4$ and $NdFe_3(BO_3)_4$ crystals (Table 1).

We used the experimental atomic coordinates of $NdGa_3(BO_3)_4$ [6], and $NdFe_3(BO_3)_4$ [22] crystals have been used as the initial ones for the calculations. There is a good agreement between the calculated and experimental data [6, 22]. Figure 3 shows energy bands located between −10.0 and 10.0 eV for $NdGa_3(BO_3)_4$ crystal.

The calculated atomic populations (Mulliken) in $NdGa_3(BO_3)_4$ crystal are presented in Table 2. The band gap is zero at Γ point in the Brillouin zone, but in point Z this band is about 0,04 eV. The bands around the Fermi level in the electronic band structure of $NdGa_3(BO_3)_4$ crystal consist mainly of p and f (Nd ions) states (Table 2). Similar calculations were performed earlier in the VASP program using the GGA: PAW potential [25]. These calculations have shown that the crystal is a dielectric with an indirect bandgap of 4.338 eV.

Figure 4 shows energy bands with geometric optimization located between −10.0 and 10.0 eV for $NdFe_3(BO_3)_4$ crystal.

The calculated atomic populations (Mulliken) in $NdFe_3(BO_3)_4$ crystal differ from the populations in the $NdFe_3(BO_3)_4$ crystal (Table 3). The bands around the Fermi level in the electronic band structure of $NdFe_3(BO_3)_4$ crystal consist mainly of *d* and f states (Fe and Nd ions). Some ab initio calculations were performed earlier in the VASP program using the GGA: PAW potential [26]. These calculations have shown that the crystal is a semiconductor with an indirect bandgap of 2.332 eV. However, the levels at the bottom of this gap are mainly formed by d electronic states of Fe. Therefore, we have to deduce that they correspond to well-known excited states of d3 ion that, as it is well established

Table 1. Lattice parameters in the *P1* phase of the compounds $NdR_3(BO_3)_4$ (R = Ga, Fe).

	$NdGa_3(BO_3)_4$	$NdFe_3(BO_3)_4$
a_{exp} (A)	6.041939 [6]	6.046 [22]
a_{calc} (A)	6.041994 [this work]	6.083 [this work]
a_{calc} (A)	6.09527734 [23–25]	6.158 [23,24, 26]
α_{exp}	103.997359 [6]	103.089 [22]
α_{calc}	103.992049 [this work]	103.85 [this work]
α_{calc}	103.84311932 [23–25]	103.753 [23,24, 26]

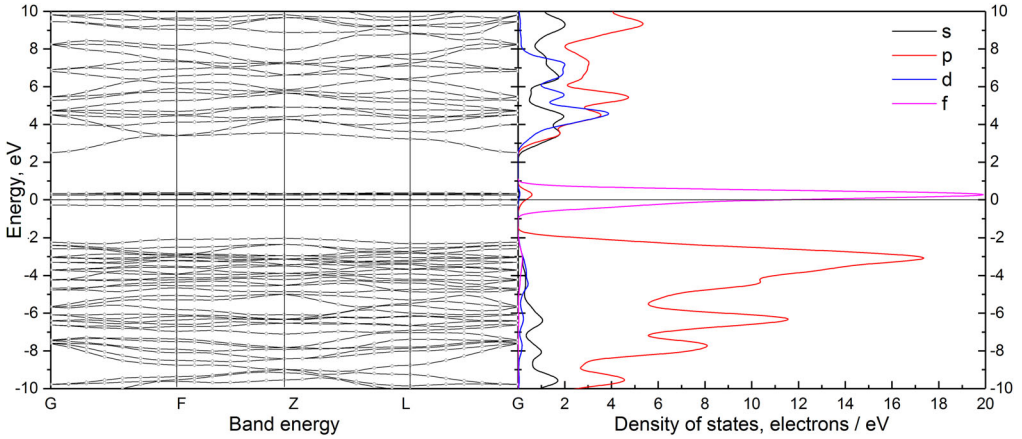

Figure 3. Calculated band structures and DOS for $NdGa_3(BO_3)_4$ with geometric optimization, no spin polarization.

Table 2. The population of $NdGa_3(BO_3)_4$ atoms calculated by Mulliken.

Species	Ion	S	p	d	f	Total
B	1	0.53	1.70	0.00	0.00	2.24
B	2	0.53	1.70	0.00	0.00	2.24
B	3	0.53	1.70	0.00	0.00	2.24
B	4	0.55	1.62	0.00	0.00	2.16
O	1	1.77	4.98	0.00	0.00	6.75
O	2	1.77	4.98	0.00	0.00	6.75
O	3	1.77	4.98	0.00	0.00	6.75
O	4	1.77	4.98	0.00	0.00	6.75
O	5	1.77	4.98	0.00	0.00	6.75
O	6	1.77	5.01	0.00	0.00	6.75
O	7	1.79	5.01	0.00	0.00	6.75
O	8	1.79	5.01	0.00	0.00	6.80
O	9	1.79	5.01	0.00	0.00	6.80
O	10	1.79	5.01	0.00	0.00	6.80
O	11	1.79	5.01	0.00	0.00	6.80
O	12	1.79	5.01	0.00	0.00	6.80
Ga	1	0.43	1.01	10.00	0.00	11.44
Ga	2	0.43	1.01	10.00	0.00	11.44
Ga	3	0.43	1.01	10.00	0.00	11.44
Nd	1	2.43	5.66	1.10	3.32	12.51

by experimental measurements of absorption spectra of ferroborates, do not form fundamental absorption edge and are observable in the form of several bands corresponding to the transitions from the ground state of Fe^{3+} ion to T, A, and E excited states of the latter.

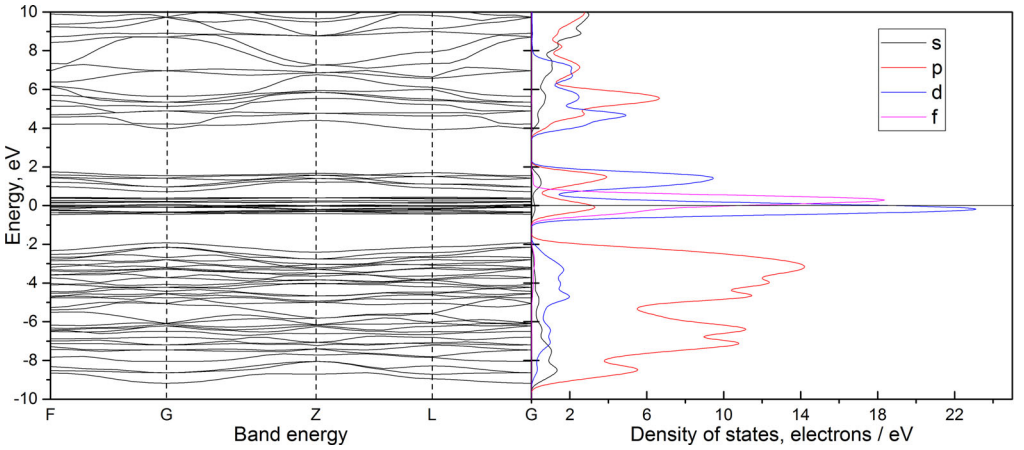

Figure 4. Calculated band structures for $NdFe_3(BO_3)_4$ with geometric optimization, no spin polarization.

Table 3. Population of $NdFe_3(BO_3)_4$ atoms calculated by Mulliken.

Species	Ion	s	p	d	f	Total
B	1	0.58	1.68	0.00	0.00	2.26
B	2	0.58	1.68	0.00	0.00	2.26
B	3	0.58	1.68	0.00	0.00	2.26
B	4	0.58	1.59	0.00	0.00	2.17
O	1	1.79	4.86	0.00	0.00	6.64
O	2	1.79	4.86	0.00	0.00	6.64
O	3	1.79	4.86	0.00	0.00	6.64
O	4	1.79	4.86	0.00	0.00	6.64
O	5	1.79	4.86	0.00	0.00	6.64
O	6	1.79	4.86	0.00	0.00	6.64
O	7	1.79	4.84	0.00	0.00	6.63
O	8	1.79	4.81	0.00	0.00	6.60
O	9	1.79	4.84	0.00	0.00	6.63
O	10	1.79	4.81	0.00	0.00	6.60
O	11	1.79	4.84	0.00	0.00	6.63
O	12	1.79	4.81	0.00	0.00	6.60
Fe	1	2.42	6.43	6.30	0.00	15.16
Fe	2	2.42	6.43	6.30	0.00	15.16
Fe	3	2.42	6.43	6.30	0.00	15.16
Nd	1	2.08	5.56	0.99	3.39	11.99

The real optical bandgap, according to Ref. [26], should be at 5 eV that contradicts to experimental results of Malakhovski et al. [27], who investigated the contribution of Fe ions to the optical spectrum of $GdFe_3(BO_3)_4$ and established that the onset of fundamental absorptions in the ferroborates occurred above 3.1 eV. The spectra of $GdFe_3(BO_3)_4$ are very similar in the range, where strong absorption due to Fe ions is pronounced since the contribution of weak *f-f* transitions is relatively small in the case of Nd. In our calculations, the levels originated from d states of Fe^{3+} ion are also predicted to be in the range of 1.5 eV. However, we observe true optical bandgap in $NdFe_3(BO_3)_4$ at $3.5 \div 4$ eV that is closer to the experiment.

4. Conclusion

The first-principles plane-wave pseudo-potential calculations with the generalized gradient approximation (GGA) with the Perdew – Burke – Ernzerhof for solids (PBE sol) functionals were carried out in order to study the electronic band structures of $NdFe_3(BO_3)_4$ and $NdGa_3(BO_3)_4$ multiferroic crystals. The calculated optimized space structures of the crystals are in good agreement with experimental data. We find that the bands near the Fermi level of both crystals include the Nd - *f* states. Fermi level in the electronic band structure of $NdFe_3(BO_3)_4$ crystal consists mainly of Fe - *d* states.

Acknowledgment

This work was supported by the Russian Foundation for Basic Research Grant No. 20-42-240009.

References

[1] A. A. Prokhorov *et al.*, Optical and magnetic properties of the ground state of Cr^{3+} doping ions in $REM_3(BO_3)_4$ single crystals, *Sci. Rep.* **9** (1), 12787 (2019). DOI: 10.1038/s41598-019-49248-0.

[2] P. Becker, Borate materials in nonlinear optics, *Adv. Mater.* **10** (13), 979 (1998). DOI: 10.1002/(SICI)1521-4095(199809)10:13 < 979::AID-ADMA979 > 3.0.CO;2-N.

[3] E. L. Belokoneva, The structures of new germanates, gallates, borates, and silicates with laser, piezoelectric, ferroelectric, and ion-conducting properties, *Russ. Chem. Rev.* **63** (7), 533 (1994). DOI: 10.1070/RC1994v063n07ABEH000103.

[4] A. M. Kadomtseva *et al.*, Magnetoelectric interactions in rare-earth ferroborates, *J. Exp. Theor. Phys.* **105** (1), 116 (2007). DOI: 10.1134/S1063776107070254.

[5] A. I. Popov, D. I. Plokhov, and A. K. Zvezdin, Quantum theory of magnetoelectricity in rare-earth multiferroics: Nd, Sm, and Eu ferroborates, *Phys. Rev. B.* **87** (2) 024413 (2013). DOI: 10.1103/PhysRevB.87.024413.

[6] E. L. Belokoneva *et al.*, Crystal structure of $NdGa_3[BO_3]_4$, *J. Struct. Chem.* **19** (2), 332 (1978). DOI: 10.1007/BF00746983.

[7] N. I. Leonyuk, and I. Leonyuk, Growth and characterization of $RM_3(BO_3)_4$ crystals, *Prog. Cryst. Growth Charact* **31** (3-4), 179 (1995). DOI: 10.1016/0960-8974(96)83730-2.

[8] C. S. Nelson, L. N. Bezmaternykh, and I. A. Gudim, Temperature- and magnetic-field-tuning of magnetic phases in multiferroic $NdFe_3(BO_3)_4$, *J. Kor. Phys. Soc* **62** (10), 1410 (2013). DOI: 10.3938/jkps.62.1410.

[9] P. Fischer *et al.*, Simultaneous antiferromagnetic Fe^{3+} and Nd^{3+} ordering in $NdFe_3(11BO_3)_4$, *J. Phys: Condens. Matter* **18** (34), 7975 (2006). DOI: 10.1088/0953-8984/18/34/010.

[10] E. P. Chukalina *et al.*, Magnetic ordering of $NdFe_3(BO_3)_4$ studied by infrared absorption spectroscopy, *Phys. Lett. A* **322** (3-4), 239 (2004). DOI: 10.1016/j.physleta.2003.12.062.

[11] D. Fausti *et al.*, Raman scattering from phonons and magnons in $RFe_3(BO_3)_4$, *Phys. Rev. B.* **74** (2), 024403 (2006). DOI: 10.1103/PhysRevB.74.024403.

[12] E. Yu. Borovikova *et al.*, Crystal growth, structure, infrared spectroscopy, and luminescent properties of rare-earth gallium borates $RGa_3(BO_3)_4$, R = Nd, Sm–Er, Y, *Opt. Mater* **49**, 304 (2015). DOI: 10.1016/j.optmat.2015.09.021.

[13] A. L. Sukhachev *et al.*, Spectroscopic properties of $HoFe_3(BO_3)_4$, $NdFe_3(BO_3)_4$ and $Ho_{0.75}Nd_{0.25}Fe_3(BO_3)_4$ single crystals, *Opt. Mater* **83**, 87 (2018). DOI: 10.1016/j.optmat.2018.05.078.

[14] A. S. Krylov *et al.*, Manifestation of magnetoelastic interactions in Raman spectra of $Ho_xNd_{1-x}Fe_3(BO_3)_4$ crystals, *J. Adv. Dielect.* **08** (02), 1850011 (2018). DOI: 10.1142/S2010135X1850011X.

[15] A. Krylov *et al.*, Low-temperature features of Raman spectra below magnetic transitions in multiferroic $Ho_{1-x}Nd_xFe_3(BO_3)_4$ and $Sm_{1-y}La_yFe_3(BO_3)_4$ single crystals, *Ferroelectrics* **509** (1), 92 (2017). DOI: 10.1080/00150193.2017.1294040.

[16] V. I. Zinenko *et al.*, Vibrational spectra and elastic, piezoelectric, and magnetoelectric properties of $HoFe_3(BO_3)_4$ and $HoAl_3(BO_3)_4$ crystals, *J. Exp. Theor. Phys.* **117** (6), 1032 (2013). DOI: 10.1134/S1063776113140203.

[17] V. A. Chernyshev *et al.*, Structure and lattice dynamics of rare-earth ferroborate crystals: Ab initio calculation, *Phys. Solid State* **58** (8), 1642 (2016). DOI: 10.1134/S1063783416080096.

[18] S. J. Clark *et al.*, First principles methods using CASTEP, *Z. Kristallogr. Cryst. Mater* **220**, 567 (2005). DOI: 10.1524/zkri.220.5.567.65075.

[19] J. P. Perdew *et al.*, Restoring the density-gradient expansion for exchange in solids and surfaces, *Phys. Rev. Lett.* **100** (13), 136406 (2008). DOI: 10.1103/PhysRevLett.100.136406.

[20] B. G. Pfrommer *et al.*, Relaxation of crystals with the quasi-Newton method, *J. Comp. Physiol* **131** (1), 233 (1997). DOI: 10.1006/jcph.1996.5612.

[21] H. J. Monkhorst, and J. D. Pack, Special points for Brillouin-zone integrations, *Phys. Rev. B.* **13** (12), 5188 (1976). DOI: 10.1103/PhysRevB.13.5188.

[22] J. A. Campa *et al.*, Crystal structure, magnetic order, and vibrational behavior in iron rare-earth borates, *Chem. Mater* **9**, 237 (1997). DOI: 10.1021/cm960313m.

[23] M. G. Vergniory *et al.*, A complete catalogue of high-quality topological materials, *Nature* **566** (7745), 480 (2019). DOI: 10.1038/s41586-019-0954-4.

[24] A. Jain *et al.*, The Materials Project: A materials genome approach to accelerating materials innovation, *APL Mater.* **1** (1), 011002 (2013). DOI: 10.1063/1.4812323.

[25] K. Persson, Materials Data on $NdGa_3(BO_3)_4$ (SG:155) by, *Materials Project*, mp-, 561187 (2014). DOI: 10.17188/1271902.

[26] K. Persson, Materials Data on $NdFe_3(BO_3)_4$ (SG:155) by, *Materials Project*, mp-, 18936 (2014). DOI: 10.17188/1193671.

[27] A. V. Malakhovskii *et al.*, Nature of optical properties of $GdFe_3(BO_3)_4$ and $GdFe_{2.1}Ga_{0.9}(BO_3)_4$ crystals and other $3d^5$ antiferromagnets, *Eur. Phys. J. B.* **85** (2), 80 (2012). DOI: 10.1140/epjb/e2012-20953-1.